NUMERICAL CONFIRMATION OF HIGH-FREQUENCY DEFECTS IN DISCRETE WAVES

LAURA JAMES
ADVISOR: HANS CHRISTIANSON

Abstract. We study the discrepancies between the continuous versus discretized wave equations. Motivated by the theoretical study of so-called "spurious" high-frequency wave packets initiated in [1], we use the finite difference algorithm to approximate solutions to a one-dimensional wave equation on $\mathbb{S}^1$ at low and high frequencies. We numerically compare these approximate solutions to the explicit continuous solutions using the discrete analog of the usual wave energy. For low frequencies there is good agreement, while for high frequencies there is very bad agreement. We explain this high frequency phenomenon heuristically by observing that, for initial data resulting in propagation in one direction only, the approximate solution nevertheless has non-trivial wave packets propagating in both directions.

1. Introduction

In this paper, we are concerned with a phenomenon which occurs with the numerical study of high frequency waves. In order to show this phenomenon, we study the wave equation on $[0, 1]$ with periodic boundary conditions using two different methods.

$$\begin{aligned} u_{tt} - u_{xx} &= 0 \\ u(t,0) &= u(t,1) \\ u_x(t,0) &= u_x(t,1) \\ u(0,x) &= f(x) \\ u_t(0,x) &= g(x) \end{aligned} \tag{1.1}$$

In the first method, we discretize on a uniform mesh with N subdivisions of length $h = \frac{1}{N}$. We use the usual finite difference matrix A and solve the resulting ODE's to get an approximation of the solution to (1.1). In the second method, we solve the wave equation in the continuum and then sample the solution on our mesh. The energy

$$E(t) = \int_0^1 (|u_t|^2 + |u_x|^2)dx \tag{1.2}$$

is known to be conserved for (1.1) (see Appendix A). If $\vec{u}$ is a discretized approximate solution, then the discrete analog of (1.2) is

$$E(\vec{u}) = \vec{u}_t \cdot \overline{\vec{u}_t} + (A\vec{u}) \cdot \overline{\vec{u}}, \tag{1.3}$$

which we use to calculate the discrete energy for the approximate solution using each method. Not surprisingly, the energy is (almost) conserved using each method. Additionally, the energy in the first method is very close to the energy in the second method. However, something interesting

occurs when we examine the energy of the difference of the two approximate solutions. For low frequencies, the energy of the difference is relatively small. On the other hand, for high frequencies the energy of the difference is much larger. This is numerical confirmation of the defects seen in high frequency discrete waves. This phenomenon was first observed numerically but the high frequencies were "truncated" (see, for example, the survey article [4] and the references therein). [1] explains theoretically what happens with these high frequencies.

1.1. **Acknowledgements.** We programmed the algorithms used in this project from scratch, which was very time consuming. Additionally, computer time was limited. Therefore, it took too much time to be able to study geometric control for the damped wave equation, which was our original motivation [1]. I would like to extend a special thanks and appreciation to my advisor Hans Christianson for his guidance on this project. Also, thank you to Jason Metcalfe, Jeremy Marzuola, and Hans Christianson for serving on the committee.

2. Descriptions of the Two Methods

2.1. **First Method.** It should be noted that we do not use any built-in functions (other than `sqrt, exp, dot`, and `zeros`) or algorithms in MATLAB, as they may have added features which we do not want in our method. In the first method, we discretize first. Our discretization occurs on a uniform mesh with N subdivisions of length $h = \frac{1}{N}$.

We use the second order finite difference matrix

$$A = \frac{1}{h^2}\begin{bmatrix} 2 & -1 & 0 & \dots & & & -1 \\ -1 & 2 & -1 & 0 & \dots & & 0 \\ 0 & -1 & 2 & -1 & 0 & \dots & 0 \\ \vdots & & & \ddots & & & \\ -1 & 0 & \dots & & 0 & -1 & 2 \end{bmatrix}$$

to approximate $\frac{-\partial^2}{\partial x^2}$ (see Appendix B).

Our discrete solution can be written as the discrete Fourier series

$$\vec{U} = \sum_j U_j \vec{e}_j \tag{2.1}$$

where

$$\vec{e}_j = \sqrt{h}\begin{bmatrix} e^{2\pi i j h * 0} \\ e^{2\pi i j h * 1} \\ \vdots \\ e^{2\pi i j h * (N-1)} \end{bmatrix}$$

is the basis of orthonormal eigenvectors of A with eigenvalues $\frac{\mu_j^2}{h^2}$

$$\begin{aligned} A\vec{e}_j &= \frac{2-2\cos(2\pi jh)}{h^2}\vec{e}_j \qquad \text{(see Appendix C)} \\ &= \frac{\mu_j^2}{h^2}\vec{e}_j \end{aligned} \tag{2.2}$$

and U_j is given by

$$U_j = \langle \vec{U}, \vec{e}_j \rangle.$$

Our wave equation then becomes the discretized wave equation

$$\vec{U}\,'' + A\vec{U} = \sum_j U_j''\vec{e}_j + \sum_j \frac{\mu_j^2}{h^2}U_j\vec{e}_j = 0 \tag{2.3}$$

with initial conditions

$$\vec{U}(0) = \vec{F}$$
$$\vec{U}\,'(0) = \vec{G}.$$

Notice that the boundary conditions are contained in A. By matching the coefficients in (2.3) we see that

$$U_j'' = -\frac{\mu_j^2}{h^2}U_j,$$

and solving this ODE gives us a formula for U_j.

$$U_j = C_{j+}e^{\frac{i\mu_j}{h}t} + C_{j-}e^{\frac{-i\mu_j}{h}t} \tag{2.4}$$

Now let's also sample our initial conditions and write them as a discrete Fourier series. We will compare to the continuum data f, g later.

$$\vec{F} = \sum_j F_j\vec{e}_j \tag{2.5}$$

$$\vec{G} = \sum_j G_j\vec{e}_j \tag{2.6}$$

Using (2.1), (2.4), (2.5), and (2.6), we obtain formulas for F_j and G_j.

$$\vec{U}(0) = \sum_j (C_{j+} + C_{j-})\vec{e}_j = \vec{F}$$

$$\vec{U}\,'(0) = \sum_j \Big(\frac{i\mu_j}{h}C_{j+} - \frac{i\mu_j}{h}C_{j-}\Big)\vec{e}_j = \vec{G}$$

Therefore,

$$F_j = C_{j+} + C_{j-} \tag{2.7}$$

$$G_j = \frac{i\mu_j}{h}C_{j+} - \frac{i\mu_j}{h}C_{j-} \tag{2.8}$$

2.2. **Second Method.** In the second method, we solve the wave equation in the continuum and then discretize. We can explicitly write out the solution as

$$u = \sum_n \Big(D_{n+} e^{2\pi i n t} + D_{n-} e^{-2\pi i n t} \Big) e^{2\pi i n x} \tag{2.9}$$

with initial conditions

$$u(0,x) = f(x) = \sum_n f_n e^{2\pi i n x} \tag{2.10}$$

$$u_t(0,x) = g(x) = \sum_n g_n e^{2\pi i n x}. \tag{2.11}$$

Using (2.9), (2.10), and (2.11), we obtain formulas for f_n and g_n.

$$u(0) = \sum_n \Big(D_{n+} + D_{n-} \Big) e^{2\pi i n x} = f(x)$$

$$u_t(0) = \sum_n \Big(2\pi i n D_{n+} - 2\pi i n D_{n-} \Big) e^{2\pi i n x} = g(x)$$

Therefore,

$$f_n = D_{n+} + D_{n-} \tag{2.12}$$

$$g_n = 2\pi i n D_{n+} - 2\pi i n D_{n-} \tag{2.13}$$

2.3. **Choice of Frequencies.** Now that we have both of our methods set up, we must determine what frequencies to use in order to illustrate the phenomenon. For our numerical experiments we need a narrow band of low frequencies as well as a narrow band of high frequencies, and both bands should not be too computationally expensive to use. The low frequency band should be near zero where the eigenvalues of both methods are very close. Therefore, we want a range where $2\pi n$ is very close to $\frac{\mu_j}{h}$. We can study the Taylor expansion of $\frac{\mu_j}{h}$ in order to determine what range to pick.

$$\begin{aligned}
\frac{\mu_j}{h} &= \frac{(2 - 2\cos(2\pi j h))^{1/2}}{h} \\
&= \frac{\sqrt{2}}{h}\Big[1 - (1 - \frac{(2\pi j h)^2}{2} + \mathcal{O}((jh)^4))\Big]^{1/2} \\
&= \frac{\sqrt{2}}{h}\Big(\frac{(2\pi j h)^2}{2}\Big)^{1/2}\Big[1 + \mathcal{O}((jh)^2)\Big]^{1/2} \\
&= 2\pi j(1 + \mathcal{O}(j^2 h^2)) \\
&= 2\pi j + \mathcal{O}(j^3 h^2)
\end{aligned}$$

Our algorithm error is $\mathcal{O}(h)$, which is the mesh size. This is one order of magnitude worse than the $\mathcal{O}(h^2)$ error in the more modern finite element method (see, for example, [3]). Therefore, a relative error in our Taylor series of $\mathcal{O}(h^{1+\epsilon})$ for $\epsilon > 0$ is sufficient as long as N is big enough. We choose $\mathcal{O}(h^2)$ because of our computer resources. Since $\mathcal{O}(j^3 h^2) = \mathcal{O}(h^2)$ if j is bounded independent of h, we arbitrarily choose to use 20 frequencies and therefore $1 \leq j \leq 20$ is our low frequency range.

For our high frequency range we choose $N-20 \leq j \leq N-1$. By periodicity, these μ_j are close to μ_j for $1 \leq j \leq 20$ and will therefore be small. However, since $2\pi n$ grows linearly in n, $2\pi n$ will be much larger than $\frac{\mu_j}{h}$ in this high frequency range. In other words, we expect good agreement of the eigenvalues in each method at low frequencies, but bad agreement at high frequencies. Our way of measuring this is to use the energy.

3. Numerical Experiments

3.1. **Low Frequency Experiments.** We now compute the low frequency approximate solution using each method, as well as compute the energy of the difference of the solutions. We write a program in MATLAB that computes all of the following equations. For simplicity we take specific frequency-localized initial data f, g. To single out the low frequencies we take

$$D_{n-} = 0 \ \forall n$$

$$D_{n+} = \begin{cases} 1, & 1 \leq n \leq 20 \\ 0, & \text{otherwise} \end{cases}$$

so that the wave only propagates in one direction. This determines f_n and g_n.

$$f_n = \begin{cases} 1, & 1 \leq n \leq 20 \\ 0, & \text{otherwise} \end{cases} \tag{3.1}$$

$$g_n = \begin{cases} 2\pi i n, & 1 \leq n \leq 20 \\ 0, & \text{otherwise} \end{cases} \tag{3.2}$$

Our solution in the continuum is therefore

$$u = \sum_{n=1}^{20} e^{2\pi i n t} e^{2\pi i n x} = \sum_{n=1}^{20} e^{2\pi i n (x+t)} \tag{3.3}$$

and

$$u_t = \sum_{n=1}^{20} (2\pi i n) e^{2\pi i n t} e^{2\pi i n x}. \tag{3.4}$$

We now discretize u by sampling it on our mesh. We call it $\vec{w}$:

$$\vec{w} = \frac{1}{\sqrt{h}} \sum_{n=1}^{20} e^{2\pi i n t} \vec{e}_n.$$

We also sample u_t and call it w_t. Notice that $\vec{w}_t$ is the same no matter if we sample u_t or take ∂_t of $\vec{w}$.

$$\vec{w}_t = \frac{1}{\sqrt{h}} \sum_{n=1}^{20} (2\pi i n) e^{2\pi i n t} \vec{e}_n.$$

We renormalize $\vec{w}$ and $\vec{w}_t$ by multiplying both equations by $\sqrt{h}$.

$$\vec{w} = \sum_{n=1}^{20} e^{2\pi i n t} \vec{e}_n \tag{3.5}$$

$$\vec{w}_t = \sum_{n=1}^{20} (2\pi i n) e^{2\pi i n t} \vec{e}_n \tag{3.6}$$

On the other hand, we sample f and g and call them $\vec{F}_1$ and $\vec{G}_1$.

$$\vec{F}_1 = \sum_{n=1}^{20} \vec{e}_n$$

$$\vec{G}_1 = \sum_{n=1}^{20} (2\pi i n) \vec{e}_n$$

This determines C_{n+} and C_{n-} in the first method and we can therefore explicitly write out $\vec{U}$ and $\vec{U}_t$.

$$C_{n+} = \frac{1}{2}\Big(1 + \frac{h}{\mu_n} \cdot 2\pi n\Big) \tag{3.7}$$

$$C_{n-} = \frac{1}{2}\Big(1 - \frac{h}{\mu_n} \cdot 2\pi n\Big) \tag{3.8}$$

$$\vec{U} = \sum_{n=1}^{20} \Big[C_{n+} e^{\frac{i\mu_n}{h} t} + C_{n-} e^{\frac{-i\mu_n}{h} t}\Big] \vec{e}_n \tag{3.9}$$

$$\vec{U}_t = \sum_{n=1}^{20} \Big[\frac{i\mu_n}{h} C_{n+} e^{\frac{i\mu_n}{h} t} - \frac{i\mu_n}{h} C_{n-} e^{\frac{-i\mu_n}{h} t}\Big] \vec{e}_n \tag{3.10}$$

Notice that for $1 \leq n \leq 20$, C_{n-} is small and therefore the wave mostly propagates in one direction. This is similar to the continuous case in (3.3), which is a function of $x + t$ and therefore propagates to the left only. We use Hamiltonian flow to explain the propagation rule $x - x_0 = \pm t$ in section 4.

Next we compute the energy of the approximate solutions at times $t = 0, \pi h, 2\pi h, \ldots, (N-1)\pi h$. The times must be irrational so that the time evolution is not periodic.

$$E(\vec{U}) = \vec{U}_t \cdot \overline{\vec{U}_t} + (A\vec{U}) \cdot \overline{\vec{U}} \tag{3.11}$$

$$E(\vec{w}) = \vec{w}_t \cdot \overline{\vec{w}_t} + (A\vec{w}) \cdot \overline{\vec{w}} \tag{3.12}$$

We run our experiments for several values of N, and we find that the energy is (almost) conserved within each method as well as between the two methods*. For example, Figure 1 shows the energy at each time using the first method and Figure 2 shows the energy at each time using the second method for $N = 2000$.

*raw data available upon request

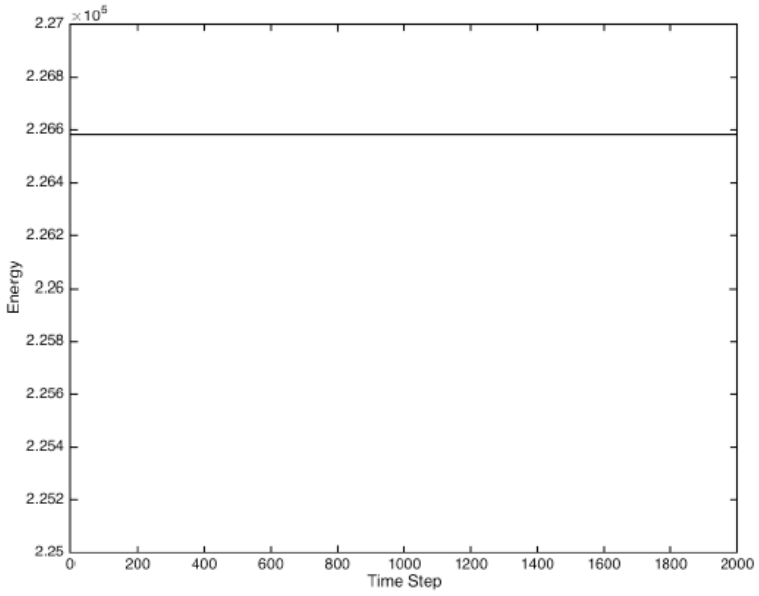

FIGURE 1. Energy of $\vec{U}$ for $N = 2000$ using the low frequency band $1 \leq n \leq 20$. The same experiment was run for $N = 100, 200, 300, \ldots, 2000, 2500, 3000, \ldots, 5000$ and the picture is similar.

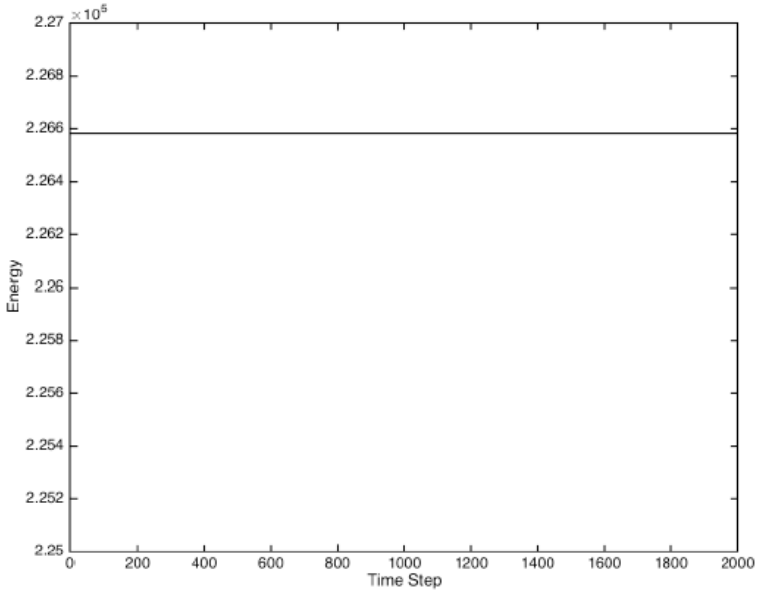

FIGURE 2. Energy of $\vec{w}$ for $N = 2000$ using the low frequency band $1 \leq n \leq 20$. The same experiment was run for $N = 100, 200, 300, \ldots, 2000, 2500, 3000, \ldots, 5000$ and the picture is similar.

We also examine the energy of the difference of the two approximate solutions.

$$E(\vec{U}-\vec{w}) = (\vec{U}_t - \vec{w}_t)\cdot\overline{(\vec{U}_t - \vec{w}_t)} + (A(\vec{U}-\vec{w}))\cdot\overline{(\vec{U}-\vec{w})} \tag{3.13}$$

We find that as N increases, the energy of the difference becomes small relative to $E(\vec{U})$. This fact is obvious when we graph the ratios $\frac{E(\vec{U}-\vec{w})((N-1)\pi h)}{E(\vec{U})((N-1)\pi h)}$ for different values of N.

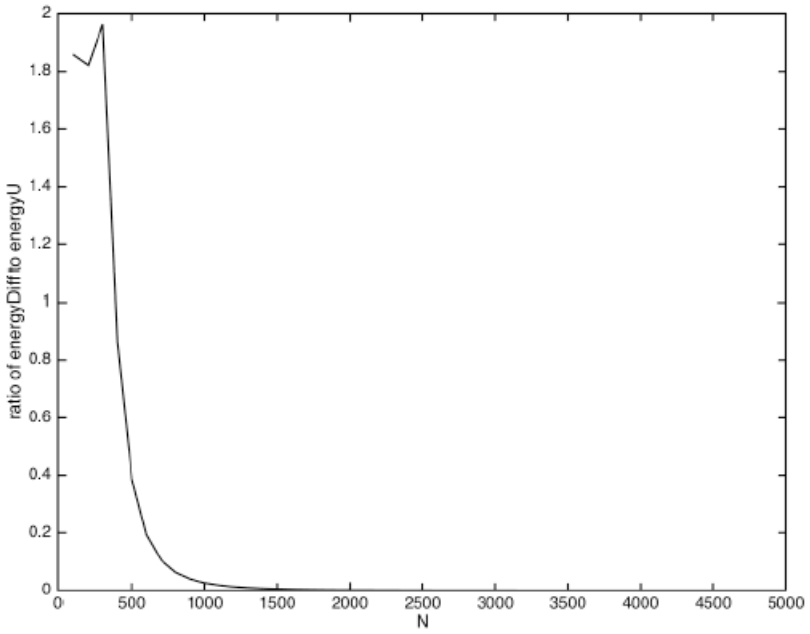

FIGURE 3. Ratio of the energy of $\vec{U}-\vec{w}$ to the energy of $\vec{U}$ at the last time step for increasing N using the low frequency band $1 \le n \le 20$. Ratios were computed for $N =$ 100, 200, 300, ... , 2000, 2500, 3000, ... , 5000.

3.2. **High Frequency Experiments.** We now run the exact same experiments with the high frequency band near N[†]. This time, C_{n-} in (3.8) is large and therefore the wave propagates in both directions. We again compute the energy of the approximate solution from each method as well as the energy of the difference. Again, we find that the energy is (almost) conserved within each method as well as between the two methods. This is shown in Figure 4 and Figure 5.

[†]raw data available upon request

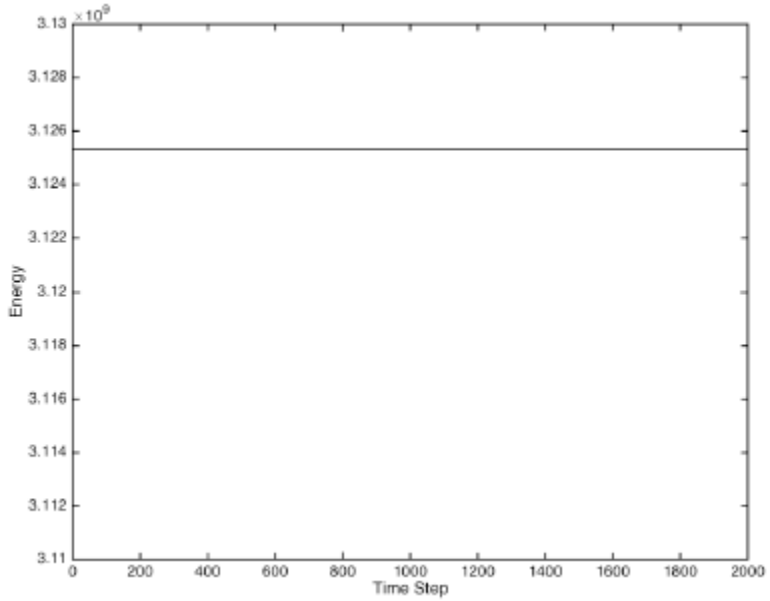

FIGURE 4. Energy of $\vec{U}$ for $N = 2000$ using the high frequency band $N-20 \leq n \leq N-1$. The same experiment was run for $N = 100$, 200, 300, ... , 2000, 2500, 3000, ... , 5000 and the picture is similar.

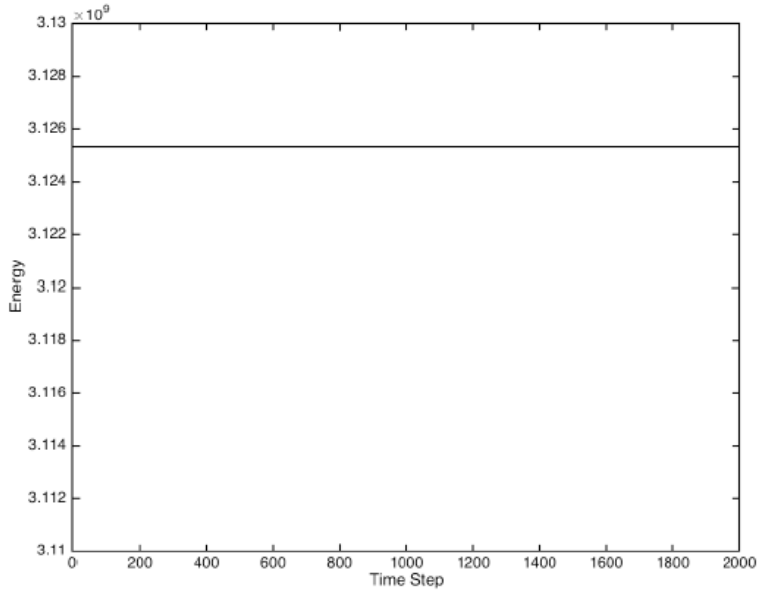

FIGURE 5. Energy of $\vec{w}$ for $N = 2000$ using the high frequency band $N-20 \leq n \leq N-1$. The same experiment was run for $N = 100$, 200, 300, ... , 2000, 2500, 3000, ... , 5000 and the picture is similar.

However, we observe that as N becomes large, the energy of the difference is on the same order of magnitude as $E(\vec{U})$. We graph the ratios $\frac{E(\vec{U}-\vec{w})((N-1)\pi h)}{E(\vec{U})((N-1)\pi h)}$, which are all order 10^0. The ratios clearly do not decay to zero as N increases.

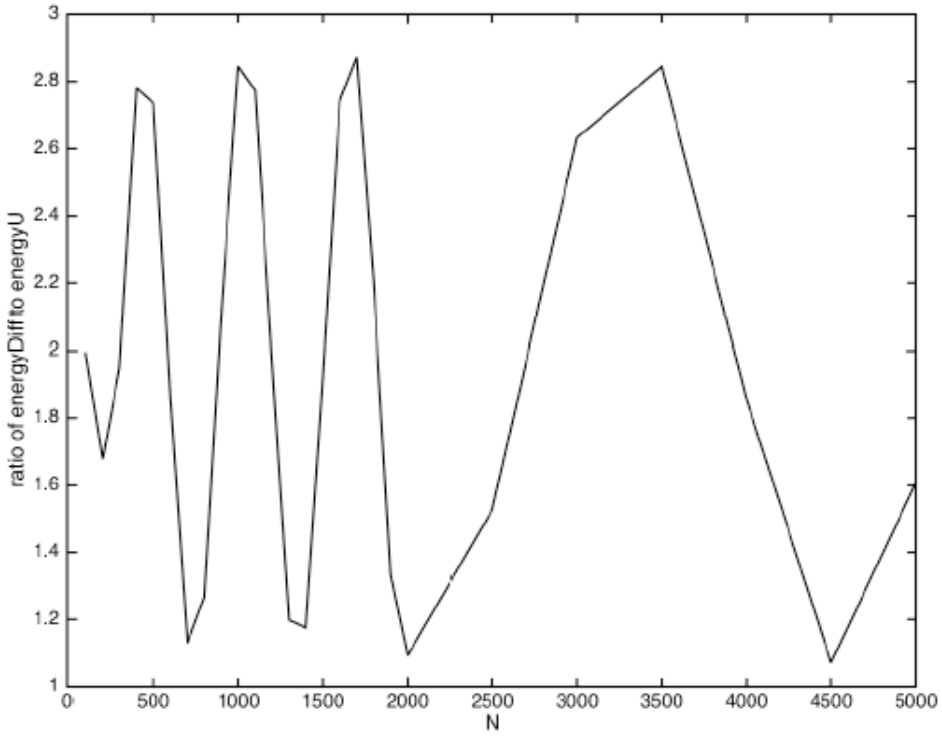

FIGURE 6. Ratio of the energy of $\vec{U} - \vec{w}$ to the energy of $\vec{U}$ at the last time step for increasing N using the high frequency band $N - 20 \leq n \leq N - 1$. Ratios were computed for $N = 100, 200, 300, \ldots, 2000, 2500, 3000, \ldots, 5000$.

4. Hamiltonian Flow

We can explain this phenomenon of defects seen in high frequency discrete waves by studying the Hamiltonian Flow of the continuous case versus the discrete case. It is well known that waves propagate along the Hamiltonian flow of the principal symbol of the wave equation, $\tau^2 - \xi^2$ [2] (See Appendix D). For low frequencies (near zero), the discrete wave propagates close to the continuous wave. However, for high frequencies (near N), propagation in the discrete case is much different than in the continuous case. The Hamiltonian in the continuum is given by

$$H^c = \tau^2 - \xi^2 \tag{4.1}$$

where $\xi = 2\pi n$ and $n \neq 0$. Our Hamiltonian ODE's are

$$\begin{aligned} \dot{\xi} &= -H_x = 0 \\ \dot{\tau} &= -H_t = 0 \\ \dot{t} &= H_\tau = 2\tau \\ \dot{x} &= H_\xi = -2\xi \end{aligned} \tag{4.2}$$

and solving gives us

$$\begin{aligned} \xi &= \xi_0 \\ \tau &= \tau_0 \\ t &= t_0 + 2\tau_0 s \\ x &= x_0 - 2\xi_0 s. \end{aligned} \tag{4.3}$$

We take $t_0 = 0$. We also avoid $\xi_0 = 0$ and $\tau_0 = 0$ so that we can solve for s.

$$s = \frac{x_0 - x}{2\xi_0} = \frac{t}{2\tau_0}$$

Waves live where $H^c = 0$ and therefore $\tau = \pm\xi$. This gives us

$$\frac{x_0 - x}{2\xi_0} = \frac{\pm t}{2\xi_0}$$

or

$$x - x_0 = \pm t. \tag{4.4}$$

Notice that the wave always has constant speed 1 no matter the frequency.

In the discrete case, our eigenvalues in (2.2) can be written as $\frac{4}{h^2}\sin^2(\pi h j)$ using trig identities. The Hamiltonian is therefore given by

$$\begin{aligned} H^d &= \tau^2 - \frac{4}{h^2}\sin^2(\pi h j) \\ &= \tau^2 - \frac{4}{h^2}\sin^2\left(\frac{h\xi}{2}\right). \end{aligned} \tag{4.5}$$

The Hamiltonian ODE's in this case are

$$\begin{aligned} \dot{\xi} &= -H_x = 0 \\ \dot{\tau} &= -H_t = 0 \\ \dot{t} &= H_\tau = 2\tau \\ \dot{x} &= H_\xi = \frac{-4}{h}\sin\left(\frac{h\xi}{2}\right)\cos\left(\frac{h\xi}{2}\right) \end{aligned} \tag{4.6}$$

and solving gives us

$$\begin{aligned} \xi &= \xi_0 \\ \tau &= \tau_0 \\ t &= t_0 + 2\tau_0 s \\ x &= x_0 - s\frac{4}{h}\sin\left(\frac{h\xi}{2}\right)\cos\left(\frac{h\xi}{2}\right). \end{aligned} \tag{4.7}$$

For low frequencies near zero,

$$\begin{aligned}\dot{x} &= \frac{-4}{h}\sin\left(\frac{h\xi}{2}\right)\cos\left(\frac{h\xi}{2}\right)\\ &= \frac{-4}{h}\sin(\pi hj)\cos(\pi hj) \rightsquigarrow \frac{-4}{h}\cdot\frac{h\xi}{2}\cdot 1 = -2\xi,\end{aligned}$$

which is equal to $\dot{x}$ in (4.2) and therefore the discrete case propagates close to the continuous case for low frequencies.

For high frequencies near N,

$$\dot{x} = \frac{-4}{h}\sin(\pi hj)\cos(\pi hj) \rightsquigarrow 0.$$

Therefore, in the discrete case propagation speed depends on frequency. Indeed for the high frequencies, there may be very little propagation at all. This is in stark contrast to the constant speed propagation seen in the continuous case. In our high frequency experiments, the propagation speed is different in the continuous case versus the discrete case. Our choice of initial data results in the wave splitting into a piece propagating to the left and a piece propagating to the right, and this is why we see large disagreement between the two methods. See the discussion around (3.8).

Appendix A. Energy Conservation for Wave Equation

We show energy conservation for the wave equation

$$u_{tt} - u_{xx} = 0$$

$$u(t,0) = u(t,1)$$

$$u_x(t,0) = u_x(t,1)$$

$$u(0,x) = f(x)$$

$$u_t(0,x) = g(x).$$

We define the energy as

$$E(t) = \int_0^1 (|u_x|^2 + |u_t|^2)dx.$$

To show energy conservation, we need to show $E'(t) = 0$. We compute

$$\begin{aligned} E'(t) &= \int_0^1 (u_x\overline{u_{xt}} + u_{xt}\overline{u_x} + u_t\overline{u_{tt}} + u_{tt}\overline{u_t})dx \\ &= 2Re\int_0^1 (u_x\overline{u_{xt}} + u_{tt}\overline{u_t})dx. \end{aligned}$$

We integrate by parts in x.

$$E'(t) = 2Re\int_0^1 (-u_{xx}\overline{u_t} + u_{tt}\overline{u_t})dx + u_x\overline{u_t}\,\Big|_0^1$$

The periodic boundary conditions

$$u(t,0) = u(t,1)$$

$$u_x(t,0) = u_x(t,1)$$

are independent of t. Hence,

$$u_t(t,0) = u_t(t,1).$$

So

$$u_x(t,0)\overline{u_t}(t,0) = u_x(t,1)\overline{u_t}(t,1)$$

and we are left with

$$\begin{aligned} E'(t) &= 2Re\int_0^1 (u_{tt} - u_{xx})\overline{u_t}dx \\ &= 0 \end{aligned}$$

using the wave equation.

Appendix B. Derivation of Second Difference Matrix A

We sample a function u on a mesh of size h to get a vector with $\frac{1}{h}$ components.

$$\vec{u} = \begin{bmatrix} u_0 \\ u_1 \\ \vdots \\ u_{N-1} \end{bmatrix}, u_j = u(jh)$$

We approximate the derivatives using difference quotients. The first derivative is approximated by

$$u'(jh) \simeq \frac{u((j+1)h) - u(jh)}{h}.$$

The second derivative is then approximated by

$$\begin{aligned} u''(jh) &\simeq \frac{u'((j+1)h) - u'(jh)}{h} \\ &= \frac{\left(\frac{u((j+1)h) - u(jh))}{h}\right) - \left(\frac{u(jh) - u((j-1)h)}{h}\right)}{h} \\ &= \frac{u((j+1)h) - 2u(jh) + u((j-1)h)}{h^2} \\ &= \frac{u_{j+1} - 2u_j + u_{j-1}}{h^2}. \end{aligned}$$

Since we are indexing $\vec{u}$ starting at zero, this formula works for $1 \leq j \leq N-2$. For $j = 0$ and $j = N-1$ we need to use the periodic boundary conditions. That is, since $u(t,0) = u(t,1)$, when we discretize we identify u_0 with u_N and u_{-1} with u_{N-1}. Thus for $j = 0$, $u_1 - 2u_0 + u_{-1} = u_1 - 2u_0 + u_{N-1}$ and similarly for $j = N-1$. Therefore,

$$\frac{-\partial^2}{\partial x^2} u \approx \frac{1}{h^2} \begin{bmatrix} 2 & -1 & 0 & \dots & & & -1 \\ -1 & 2 & -1 & 0 & \dots & & 0 \\ 0 & -1 & 2 & -1 & 0 & \dots & 0 \\ \vdots & & & \ddots & & & \\ -1 & 0 & \dots & & 0 & -1 & 2 \end{bmatrix} \vec{u}.$$

Appendix C. Eigenvalues of Matrix A

We define the vectors $\vec{e_j}$ to be

$$\vec{e}_j = \sqrt{h} \begin{bmatrix} e^{2\pi i j h * 0} \\ e^{2\pi i j h * 1} \\ \vdots \\ e^{2\pi i j h * (N-1)} \end{bmatrix}.$$

The $\sqrt{h}$ factor makes the vectors orthonormal, that is

$$\vec{e_j} \cdot \overline{\vec{e_k}} = \delta_{jk}.$$

We apply matrix A to $\vec{e_j}$:

$$A\vec{e_j} = \frac{1}{h^2}\begin{bmatrix} 2 & -1 & 0 & \dots & & & -1 \\ -1 & 2 & -1 & 0 & \dots & & 0 \\ 0 & -1 & 2 & -1 & 0 & \dots & 0 \\ \vdots & & & \ddots & & & \\ -1 & 0 & \dots & & 0 & -1 & 2 \end{bmatrix} \sqrt{h}\begin{bmatrix} e^{2\pi ijh*0} \\ e^{2\pi ijh*1} \\ \vdots \\ e^{2\pi ijh*(N-1)} \end{bmatrix}$$

The kth entry is

$$\begin{aligned}(A\vec{e_j})_k &= \sqrt{h}\left[\frac{-(e^{2\pi ijh})^{k-1} + 2(e^{2\pi ijh})^k - (e^{2\pi ijh})^{k+1}}{h^2}\right] \\ &= \sqrt{h}\left[\frac{-e^{2\pi ijhk}e^{-2\pi ijh} + 2e^{2\pi ijhk} - e^{2\pi ijhk}e^{2\pi ijh}}{h^2}\right] \\ &= \sqrt{h}\left[\frac{(2 - e^{-2\pi ijh} - e^{2\pi ijh})e^{2\pi ijhk}}{h^2}\right]\end{aligned}$$

Notice

$$\begin{aligned}e^{-2\pi ijh} + e^{2\pi ijh} &= (\cos(-2\pi jh)) + i\sin(-2\pi jh)) + (\cos(2\pi jh) + i\sin(2\pi jh)) \\ &= 2\cos(2\pi jh).\end{aligned}$$

So

$$(A\vec{e_j})_k = \sqrt{h}\left[\frac{2 - 2\cos(2\pi jh))}{h^2}e^{2\pi ijhk}\right]$$

and therefore

$$A\vec{e_j} = \frac{2 - 2\cos(2\pi jh)}{h^2}\vec{e_j}.$$

In other words, the collection $\{\vec{e_j}\}$ are eigenvectors with eigenvalues $\left\{\frac{\mu_j^2}{h^2}\right\} = \left\{\frac{2-2\cos(2\pi jh)}{h^2}\right\}$. Hence they constitute an orthonormal basis of $\mathbb{R}^N$ of eigenvectors of the matrix A.

Appendix D. Derivation of Symbols

Fourier series replaces differentiation with multiplication. Take, for example, the Fourier series of a function $G(x)$.

$$G(x) = \sum_n G_n e^{2\pi inx}$$

$$G_n = \langle G(x), e^{2\pi inx}\rangle$$

If we differentiate $G(x)$ twice, we get:

$$\begin{aligned}\partial_x^2 G(x) &= \sum_n G_n(2\pi in)^2 e^{2\pi inx} \\ &= \sum_n -(2\pi n)^2 G_n e^{2\pi inx}\end{aligned}$$

We replace $2\pi n$ with the continuous variable ξ, and therefore the symbol for ∂_x^2 is $-\xi^2$.

For the wave equation, we take:

$$\begin{aligned}(\partial_t^2 - \partial_x^2)u(t,x) &= (\partial_t^2 - \partial_x^2)\sum_n u_n(t)e^{2\pi inx} = 0\\ &= \partial_t^2 \sum_n u_n(t)e^{2\pi inx} + \sum_n (2\pi n)^2 u_n(t)e^{2\pi inx}\\ &= \sum_n [u_n''(t) + (2\pi n)^2 u_n(t)]e^{2\pi inx}\end{aligned}$$

Therefore for each n,

$$\partial_t^2 u_n(t) + (2\pi n)^2 u_n = 0.$$

We take the Fourier transform in time:

$$\mathcal{F}(\partial_t^2 u_n(t) + (2\pi n)^2 u_n) = \frac{1}{\sqrt{2\pi}}\int_{-\infty}^{\infty} e^{-i\tau t}(\partial_t^2 u_n(t) + (2\pi n)^2 u_n)dt = 0$$

To solve this integral, we formally integrate by parts twice:

$$\begin{aligned}&= \frac{1}{\sqrt{2\pi}}\int_{-\infty}^{\infty} -\partial_t e^{-i\tau t}\partial_t u_n + e^{-i\tau t}(2\pi n)^2 u_n dt\\ &= \frac{1}{\sqrt{2\pi}}\int_{-\infty}^{\infty} \partial_t^2 e^{-i\tau t} u_n + e^{-i\tau t}(2\pi n)^2 u_n dt\\ &= \frac{1}{\sqrt{2\pi}}\int_{-\infty}^{\infty} [-\tau^2 u_n + (2\pi n)^2 u_n]e^{-i\tau t}dt\end{aligned}$$

This is the definition of the Fourier transform of $-\tau^2 u_n + (2\pi n)^2 u_n$. Hence,

$$-\tau^2 \hat{u}_n + (2\pi n)^2 \hat{u}_n = (-\tau^2 + \xi^2)\hat{u}_n = 0$$

Therefore the symbol for the wave equation in the continuum is

$$-\tau^2 + \xi^2$$

or

$$\tau^2 - \xi^2.$$

For the discrete case, we have

$$(\partial_t^2 + A)\vec{U} = 0$$

or

$$\sum_n (\partial_t^2 + A)U_n(t)\vec{e_n} = \sum_n U_n''\vec{e_n} + \sum_n \frac{\mu_n^2}{h^2}U_n\vec{e_n} = 0.$$

Now the eigenvalues are $\frac{\mu_n^2}{h^2} = \frac{4}{h^2}\sin^2(\pi hn)$ instead of $(2\pi n)^2$. Hence, the symbol for the wave equation in the discrete case is

$$\tau^2 - \frac{4}{h^2}\sin^2(\pi hn)$$

or

$$\tau^2 - \frac{4}{h^2}\sin^2(\frac{h\xi}{2}).$$

References

[1] H. Christianson and F. Macìa. Semiclassical measures and observability for discrete waves. *in preparation*, 2016.
[2] L. Hörmander. Fourier integral operators. I. *Acta Math.*, 127(1-2):79–183, 1971.
[3] G. Strang. *Computational science and engineering*. Wellesley-Cambridge Press, Wellesley, MA, 2007.
[4] E. Zuazua. Propagation, observation, and control of waves approximated by finite difference methods. *SIAM Rev.*, 47(2):197–243 (electronic), 2005.